

This is the author version of an article published as:

**Liaghati, Tania and Cox, Malcolm E. and Preda, Micaela (2005)
Distribution of Fe in waters and bottom sediments of a small
estuarine catchment, Pumicestone Region, southeast Queensland,
Australia. Science of The Total Environment 336(1-3):pp. 243-254.**

Copyright 2005 Elsevier

Accessed from <http://eprints.qut.edu.au>

**PAPER 4 - DISTRIBUTION OF Fe IN WATERS AND BOTTOM
SEDIMENTS OF A SMALL TIDAL CATCHMENT, PUMICESTONE
REGION, SOUTHEAST QUEENSLAND, AUSTRALIA**

Tania Liaghati, Malcolm E. Cox, Micaela Preda

School of Natural Resource Sciences
Queensland University of Technology (QUT)

The Science of Total Environment (accepted for publication)

Abstract

Dissolved and extractable iron concentrations in surface water, groundwater and bottom sediments were determined for Halls Creek, a small subtropical tidally influenced creek. Dissolved iron concentrations were much higher in fresh surface waters and groundwater compared to the estuarine water. In bottom sediments, iron minerals were determined by x-ray diffraction; of these, hematite (up to 11%) has formed by precipitation from iron-rich water in the freshwater section of the catchment. Pyrite was only identified in the estuarine reach and demonstrated several morphologies (identified by scanning electron microscopy) including loosely and closely packed framboids, and the euhedral form. The forms of pyrite found in bottom sediments indicate *in situ* production and recrystallisation. In surface waters, pyrite was detected in suspended sediment; due to oxygen concentrations well above 50 $\mu\text{mol/L}$, it was concluded that framboids do not form in the water column but are within resuspended bottom sediments or eroded from creek banks. The persistence of framboids in suspended sediments, where oxygen levels are relatively high, could be due to their silica and clay-rich coatings, which prevent a rapid oxidation of the pyrite.

In addition to identifying processes of formation and transport of pyrite, this study has environmental significance, as this mineral is a potential source of bioavailable forms of iron, which can be a major nutrient supporting algal growth.

Keywords: iron, surface water, bottom sediments, suspended sediments, pyrite framboids

INTRODUCTION

1. Introduction

Estuaries are dynamic environments, which depending on their geomorphology and hydrological regime can effectively trap catchment-derived sediment. This material includes minor and trace metals derived from the weathering of rocks and anthropogenic sources (Martin and Windom, 1991; Zwolsman et al., 1996). Among these metals, iron is an important biological and geochemical trace element in estuarine ecosystems; however, excess iron is of environmental concern in these settings due to biogeochemical recycling and ecological risks (e.g. major nutrient for algae blooms) (e.g. Liu et al., 2003). Furthermore, it is currently recognised that the chemical speciation and distribution of iron are not yet fully understood (Kuma et al., 1998).

In oxic seawater, iron is present predominantly in the insoluble and thermodynamically stable 3^+ oxidation state (Morel and Hering, 1993; Stumm and Morgan, 1996). In coastal environments such as estuaries, pH and salinity are often similar to the open sea, even though input of iron is much higher than to the oceans. Consequently, insoluble ferric oxyhydroxides are usually the stable product of chemical transformations involving iron; therefore, iron may still be scarce in these environments from a biological perspective (Rose and Waite, 2003).

Iron has been identified as an important limiting nutrient in plankton productivity (Martin et al., 1990; Croot and Hunter, 2000), and in particular, cyanobacterial productivity (Pearl et al., 1987). Recent studies in the Pumicestone region of southeast Queensland (Figure 1) have identified iron as one of the main elements supporting the growth of *Lyngbya majuscula*, a filamentous marine cyanobacterium that is often found attached to the sea floor, sea grass or rock outcrops. *Lyngbya* is toxic and negatively affects the aquatic fauna (Dennison and Abal, 1999). While the effect of iron and other macronutrients such as N and P has been well established throughout the Pumicestone and adjacent Moreton Bay regions (Dennison and Abal, 1999; Watkinson, 2000; Ahern et al., 2003), a geochemical and mineralogical study focused on identifying iron species and their source is lacking. This study, therefore,

aims to identify the source and elucidate the path of iron transport from its source to surface and groundwater, suspended material and bottom sediments.

In a previous study of the regional sediment geochemistry, pyrite was found in estuarine sediments (Liaghati et al., 2003). In this study, we examine the morphology and likely source of this iron sulfide mineral. Pyrite commonly forms under reducing waterlogged conditions where sulfur and iron are present. Disturbance of such environments and subsequent oxidation of pyrite can lead to the production of sulfuric acid, which can have a detrimental impact on the environment, and release toxic metals and bioavailable Fe^{2+} . Although many studies have addressed issues related to the occurrence and formation of sedimentary pyrite (e.g. Rickard, 1973; Lord and Church, 1983; Berner, 1984; Wada and Seisuwani, 1988; Dent and Pons, 1995), there is limited information on the size and morphology of the crystalline form of pyrite termed framboidal pyrite, which is indicative of the conditions under which the pyrite crystals have formed (Middleburg et al., 1988; Skei, 1988; Sawlowicz, 2000).

In this study we examine the concentration and distribution of dissolved iron in water and sediments, the iron minerals contained in bottom sediments, their source and migration path, and variations in the morphology of pyrite present in the bottom and suspended sediments.

The study site is located in the Pumicestone Region of southeast Queensland, on the north-western margin of Moreton Bay (Figure 1). The study area is the small tidally influenced catchment of Halls Creek (Figure 2), which drains the coastal plain into Pumicestone Passage estuary, which is connected to Moreton Bay. The catchment is low lying, <10 m above sea level, and consists of Quaternary age sediments overlying sandstone bedrock (Liaghati et al., 2003).

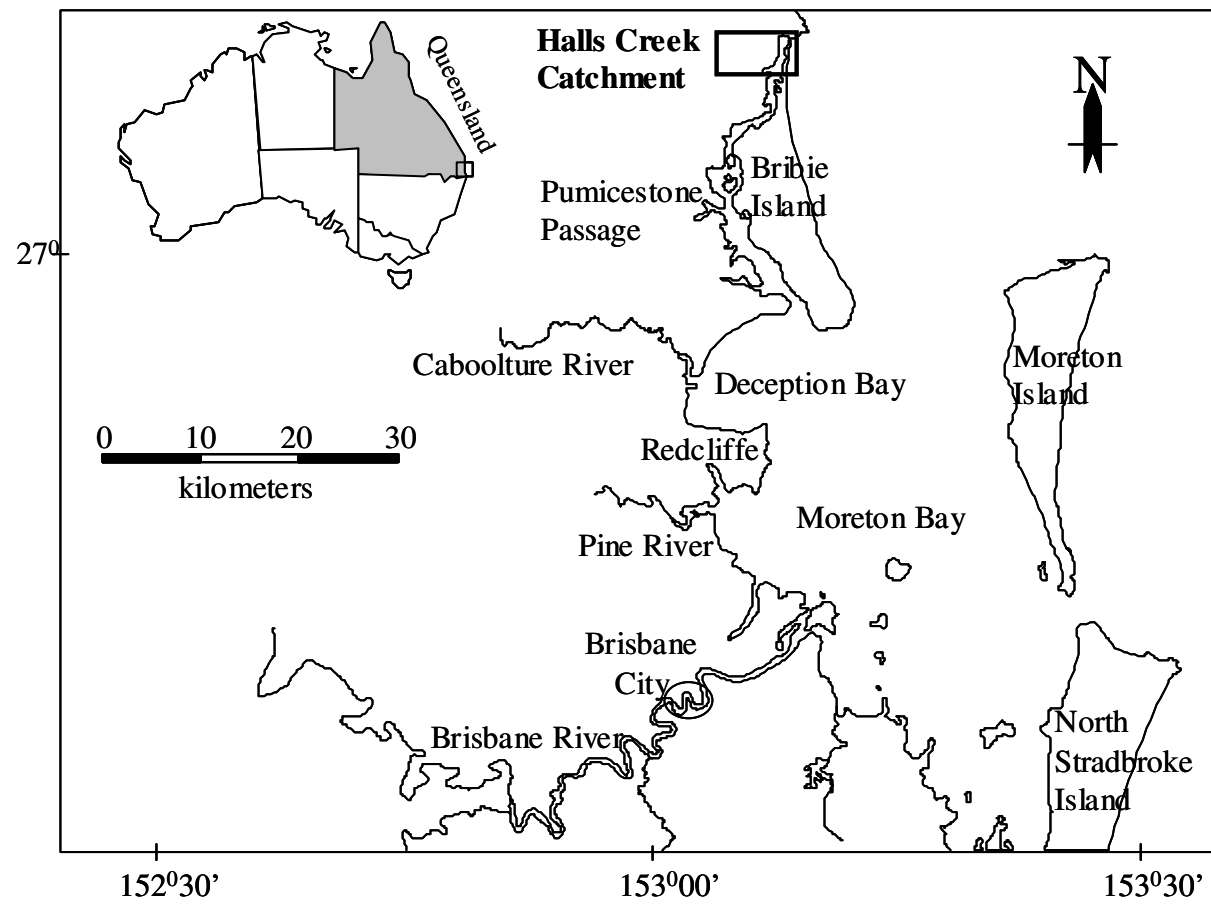


Figure 1: Location of the study area with relation to Pumicestone and Moreton Bay area.

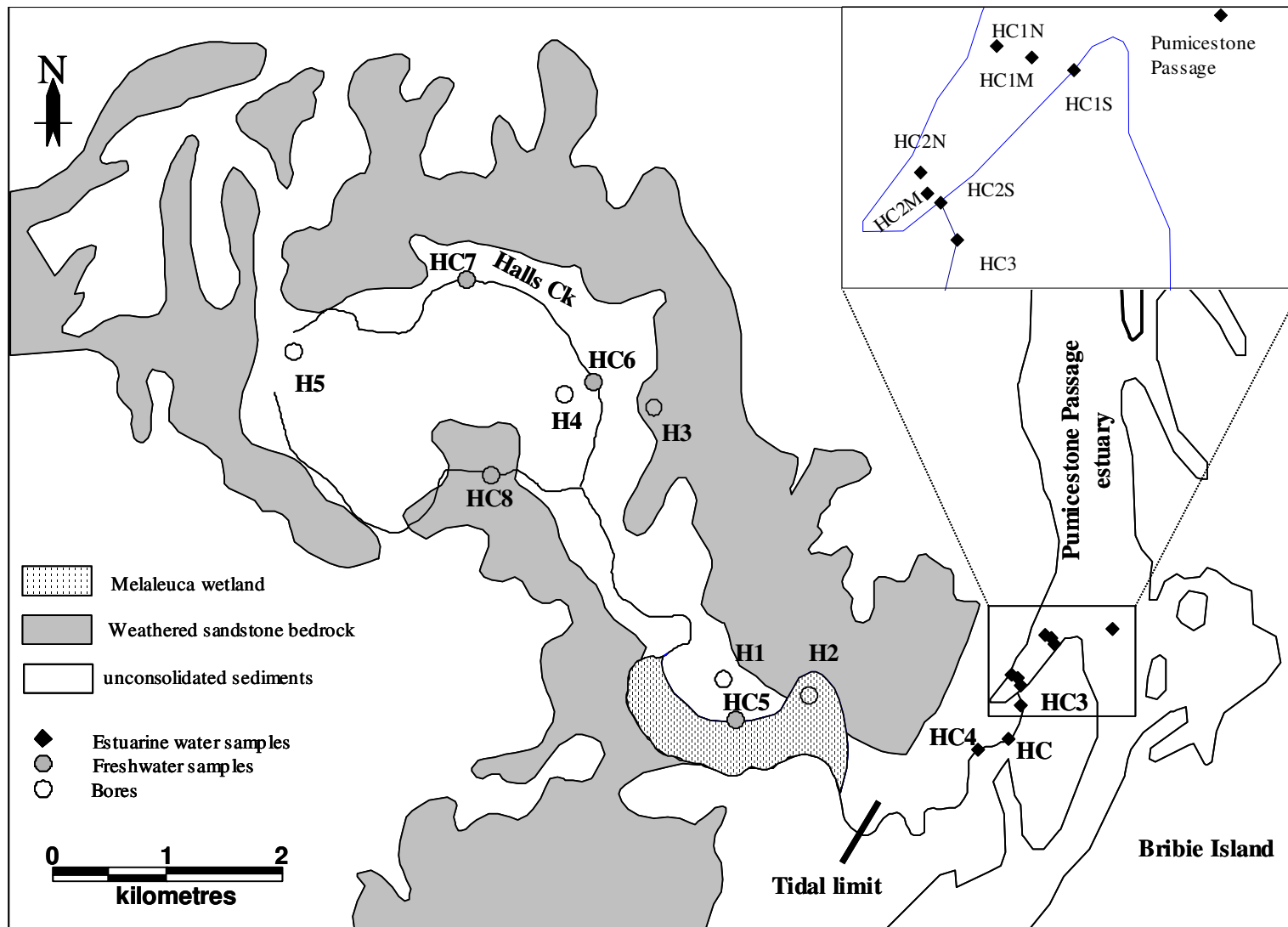


Figure 2: Location of Halls Creek catchment, details of drainage system and main lithology. Sample location and type are shown (after NSR Environmental Consultants, 1999)

2. Material and methods

2.1. Sampling Strategy

To identify the source and migration of metals in Halls Creek catchment and to better understand the processes involved in the transportation of metals, samples were collected from surface and groundwater, as well as bottom sediments. Samples of a floating ‘film’ of suspended sediment were also collected from surface waters. This small catchment was selected as the study site as ‘iron staining’ has been observed on both the creek banks and in the adjacent wetlands, suggesting that in this creek there may be relatively high levels of iron in the water column and sediments.

The samples of surficial fluvial alluvium and estuarine sediment (top ~ 5 cm of undisturbed sediment) were collected using a 0.5 litre Van Veen-type grab sampler. Samples of stream water (10 cm depth) and groundwater from bores were collected in April 2003, one week after a heavy rainfall event (74 mm over 2 days, Queensland Department of Primary Industry–Forestry, unpublished data, 2003). Groundwater samples were collected from 5 bores (constructed and maintained by School of Natural Resource Sciences, Queensland University of Technology) by submersible bailers. Samples were immediately chilled and analysed within 48h of collection. The samples for cation analyses were collected in polyethylene bottles aged in nitric acid for at least 4 days; samples for anion analyses were collected in non-acidified bottles. The water samples were filtered using a 45µ filter and refrigerated; electrical conductivity (EC), dissolved oxygen (DO) and pH were measured in the field with a TPS 90FL meter.

2.2. Analytical Methods

2.2.1. Water samples

Cation analysis was conducted using inductively coupled plasma optical emission spectroscopy (ICP-OES), which was calibrated against appropriate standards and a blank prepared with nitric acid. Anions were determined by ion chromatography (IC) and the alkalinity as HCO_3^- by titration with 0.02 N standard HCl following procedures described in Greenberg et al. (1992). Selected water samples were filtered and the form and composition of particulate matter was analysed using a FEI Quanta 200 Environmental SEM and JEOL 840A Electron Probe Micro-analyser.

2.2.2. Bottom sediment samples

The mineral composition of sediments was determined using x-ray diffraction (Philips PW 1050 diffractometer equipped with a cobalt anode). Bulk (non-oriented) powder samples were used to obtain total composition; oriented specimens were prepared for clay identification. The preparation of oriented samples exploits the sheet structure of the clay minerals and produces a pseudo-macrocrystal with a more intense diffraction pattern. The quantification of mineral phases was assisted by SIROQUANT (quantification program which expresses the composition of crystalline material within a sample in percentage of dry weight). Selected bottom sediment samples were examined for presence and form of pyrite using a FEI Quanta 200 Environmental Scanning Electron Microscope (SEM).

The extractable iron was analysed by digesting the sediment samples in aqua regia (1 HNO₃: 3 HCl) following a procedure described by Loring and Rantala (1992); quantification was by ICP-OES.

3. Results and discussion

3.1. Water chemistry

3.1.1. Major elements

The chemical composition of natural water sampled in and around Halls Creek is presented in Table 1. The water samples were classified based on their total dissolved solids (TDS) as fresh, brackish and saline. The major element composition of all the water samples is Na-Cl. The freshwater section of the creek is typically acidic to neutral (pH 5-7), and the lower estuarine reach sampled is alkaline (pH 7-8). Electrical conductivity varied between 0.1 and 0.7 mS/cm for the freshwater section (surface and groundwater) and between 17 and 30 mS/cm for the estuarine section. The groundwater is generally fresh with the exception of bore H1, where both freshwater flushing and saltwater intrusion have been found to occur (Ezzy and Cox, 2003).

The major sources of soluble elements in a river system usually include: (1) sea salts carried inland in the atmosphere and deposited in the river (cyclic salts), (2) weathering products of silicate and sulfide minerals, and (3) anthropogenic input

(Berner and Berner, 1996). Land-use in this non-industrialised catchment is semi-rural with pine plantations, therefore, only sources (1) and (2) are likely to be dominant. Gibbs (1970) suggested that a simple plot of TDS versus the weight ratio of $\text{Na}^+(\text{Na}^+ + \text{Ca}^{2+})$ can provide insights into the relative importance of the major natural mechanisms controlling surface and groundwater chemistry such as atmospheric precipitation, rock weathering and evaporation and fractional crystallisation. While Gibbs's method is known to be less clear for waters with high $\text{Na}^+(\text{Na}^+ + \text{Ca}^{2+})$ (Gibbs, 1970; Berner and Berner, 1996; Faure, 1998), it otherwise provides a useful method to identify processes affecting the chemistry of waters that are dominated by the influence of rock weathering (Berner and Berner, 1996).

For Halls Creek, the plot of TDS concentrations of the surface and groundwater samples and their weight ratios of $\text{Na}^+(\text{Na}^+ + \text{Ca}^{2+})$ (Figure 3) shows that these waters are characterised by a high ratio of $\text{Na}^+(\text{Na}^+ + \text{Ca}^{2+})$, approaching 1. Overall, while the contribution of atmospheric precipitation is zero, both evaporation and weathering are shown to be principal contributors to the major element geochemistry of water samples (Figure 3).

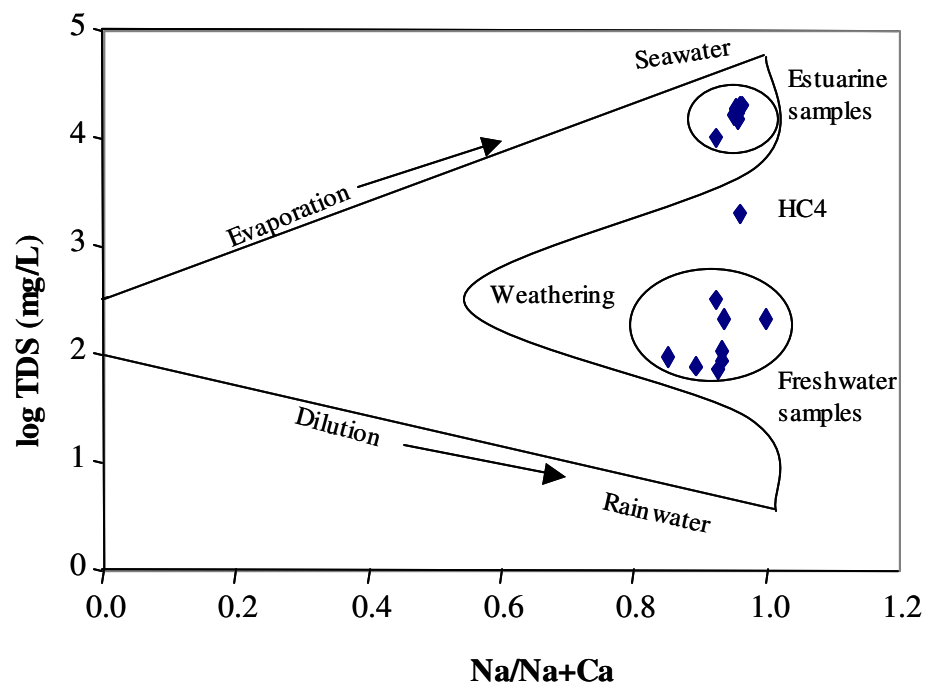


Figure 3: Classification of water samples according to Gibbs (1970). Water chemistry in the central part of the “boomerang” is dominated by weathering of silicate minerals. Samples in the upper part of the boomerang represent progressive evaporation resulting in an increase in TDS and enrich the water in Na^+ while depleting in Ca^{2+} . The lower part of the diagram represents water

Table 1: Chemical character of surface and groundwater in Halls Creek catchment

(values are in mg/L, unless otherwise specified).

Samples	Water type	Depth Sampled (m)	Groundwater aquifer type	pH	Cond mS/cm	DO	TDS	Na	K	Mg	Ca	Mn	Fe	Al	HCO ₃	SO ₄	Cl	Salinity ₁
HC8	SWF	0.1	..	6.0	0.145	2.4	69	18	1	3	2	0.01	1.24	0.29	1	3	35	fresh
HC7	SWF	0.1	..	6.0	0.131	2	77	26	1	3	3	0.03	3.54	0.96	2	1	31	fresh
HC6	SWF	0.1	..	5.0	0.156	1.6	105	28	0	3	2	0.02	2.42	0.49	3	7	46	fresh
HC5	SWF	0.1	..	7.0	0.747	3	95	18	3	2	4	0.04	8.93	0.67	9	4	36	fresh
HC4	SWE	0.1	..	7.2	21.8	4.6	2002	631	27	75	26	0.05	15.7	0.27	70	140	1007	brackish
HC3	SWE	0.1	..	7.7	27.7	6.5	19656	5533	281	791	214	0.03	0.87	0.38	141	1376	11279	fresh
HC2M	SWE	0.1	..	7.8	28.1	6.5	17534	4360	220	571	186	0.04	0.95	0.23	148	1298	9492	saline
HC2S	SWE	0.1	..	7.7	27.7	6.8	15032	4225	226	575	188	0.04	0.69	0.14	143	1191	8411	saline
HC2N	SWE	0.1	..	7.4	25.4	5.9	16331	3718	196	504	166	0.06	1.76	0.43	132	1229	9066	saline
HC1M	SWE	0.1	..	7.9	29.8	7.3	16407	4388	239	607	201	0.02	0.3	0.22	147	1552	9222	saline
HC1S	SWE	0.1	..	7.9	29.3	7.3	15985	4180	252	630	208	0.03	0.43	0.18	144	1357	9173	saline
HC1N	SWE	0.1	..	7.7	28.6	6.2	18414	4075	227	590	191	0.04	0.86	0.24	143	1436	10443	saline
H5	GW	~10	WB	7.6	0.094	6.7	90	29	0	1	2	0.05	0.13	0.42	6	4	35	fresh
H4	GW	~10	WB	6.4	0.41	5	208	65	0	1	0	0	0.47	0.11	6	111	26	fresh
H3	GW	~10	WB	7.8	0.207	2.8	208	60	3	4	4	0.07	1.44	2.83	18	33	90	fresh
H1	GW	~10	A	6.2	17.3	3.4	10195	2706	115	477	220	0.27	6.11	0.3	1220	1536	4557	saline
H2	GW	~10	A	5.9	0.586	2.8	314	86	6	10	7	0.06	6.53	0.29	5	36	151	fresh

Salinity classification using total dissolved solids (TDS) after Gorrell, (1953).

Fresh <1000

Brackish 1000-10,000

Saline 10,000-100,000

Brine >100,000

SWF = fresh surface water; SWE = estuarine surface water; GW = groundwater; WB = weathered bedrock; A = alluvial material

3.1.2. Minor elements

The content of minor elements such as Mn and Al is very low in waters sampled and does not exceed 0.3 and 2.8 mg/L, respectively (Table 1). It has been observed that the solubility of Al is strongly pH dependent and significant environmental concentration is only found below pH 5.5 where an increasing concentration is due to the solubility of microcrystalline gibbsite (Bache, 1986). At a pH of >5, it is not likely that unstable, toxic forms of Al will be present in natural waters, although colloidal aluminium and other aluminosilicate colloids may contribute to the total aluminium in waters (Edmunds and Smedley, 1996).

The concentration of iron, however, is high in Halls Creek, with maximum concentrations of 8.9 mg/L in the freshwater section and 15.7 mg/L at site HC4, the boundary between the fresh and saline sections of the study area. The sudden drop in Fe content from site HC4 (15.7 mg/L) to HC3 (0.87 mg/L) may be due to the inorganic removal of “dissolved” iron in the estuary (e.g. Liss, 1976; Boyle et al., 1977; Aston, 1978; Burton, 1988); when freshwater with a pH of around 5 reaches the saline estuary water with a pH around 7.9, there appears to be rapid precipitation of dissolved iron. This process was also observed by Crerar et al. (1981) who found that with an increase of pH during the mixing of freshwater with seawater, the dissolved inorganic Fe becomes supersaturated and precipitates as Fe oxyhydroxides floccules along with the pre-existing Fe colloids and high molecular weight humic material.

3.2. *Bottom sediments*

3.2.1. Mineralogy

The most abundant primary minerals detected in the bottom sediment samples are quartz (33-100%) followed by feldspars (up to 14%; Table 2). The clay component varies largely and consists of kaolinite (traces-53%), smectite-illite mixed layer (up to 11%) and illite (up to 4%).

Minerals such as pyrite and hematite also occur in some samples and have distinct spatial distributions. While pyrite was only found within the estuarine section, hematite is only present in the upper fresher part of the creek. Pyrite and hematite have been previously reported throughout the catchment (Liaghati et al., 2003),

however, the amounts reported were significantly lower (0.8 and 2% for pyrite and hematite, respectively) than within the Halls Creek catchment (2.6 and 11% for pyrite and hematite, respectively; Table 2).

Table 2: Mineralogy of bottom sediments (%)

Sample	Quartz	Feldspars	Kaolinite	Illite-smectite	Illite	Pyrite	Hematite
HC8	62.1	traces	28.1	0.0	0.0	0.0	9.8
HC7	100.0	0.0	traces	0.0	0.0	0.0	0.0
HC6	71.6	0.3	16.9	0.0	0.0	0.0	11.2
HC5	66.5	1.0	19.7	0.0	3.8	0.0	9.0
HC4	33.2	11.0	53.1	0.0	0.0	2.6	0.0
HC3	47.7	9.7	40.4	0.0	0.0	2.2	0.0
HC	42.2	14.4	32.0	11.4	0.0	0.0	0.0
HC2M	85.0	3.1	7.7	0.1	2.5	1.5	0.0
HC2S	76.4	4.9	13.9	0.2	2.3	2.2	0.0
HC2N	86.1	2.9	8.0	0.1	2.0	1.0	0.0
HC1M	54.8	11.2	24.9	3.9	3.6	1.5	0.0
HC1S	81.3	6.0	10.6	0.4	0.6	1.1	0.0
HC1N	90.6	2.6	3.7	0.1	2.0	1.1	0.0

Secondary minerals such as hematite are commonly formed by sulfide oxidation or precipitation from metal-rich water. As the pH of the creek water increases downstream, due to estuarine mixing, secondary minerals can precipitate as streambed deposits (e.g. Swayze et al., 1996). In the study area, however, hematite was identified (9-11%) only in the freshwater section where the pH ranged between 5 and 7, suggesting that the precipitation of hematite was from iron-rich water. The dominant source of iron in the Halls Creek catchment is the Landsborough Sandstone bedrock (Liaghati et al., 2002).

In aquatic sediments, bacteria degrade organic matter aerobically with oxygen as an electron acceptor. When all oxygen is depleted, iron oxides act as solid-phase electron acceptors for anaerobic degradation of organic matter. Both the aerobic and anaerobic degradation pathways have been intensively studied (e.g. Jorgensen, 1977; Canfield et al., 1993a; Canfield et al., 1993b). It is most likely therefore, that with high organic carbon loadings throughout the study area (up to 10%, Liaghati et al., 2003), the above biogeochemical process is responsible for iron oxide reduction and the release of Fe^{2+} to the lower saline section of the study area (e.g. Canfield, 1989;

Canfield, 1994; Wijsman et al., 2001). The presence of sulfate (SO_4^{2-}) from seawater, iron from the reduction of hematite and organic material, therefore, appear to have resulted in the formation of sedimentary pyrite.

3.2.2. Pyrite morphology

Erosion of streambeds and banks can result in the presence of organic and inorganic phases of iron minerals in streams. For example, suspended sediment samples collected from the surface of river water at the southern margin of Moreton Bay contained clay particles, amorphous iron phases and well-developed crystals of jarosite (Preda and Cox, 2000). Similar suspended sediment was observed in this study. The slightly orange, oily film on the surface of water in Halls Creek was collected at sites H2 and HC, while bottom sediment samples were collected from adjacent sites (HC3 and HC4, Figure 2). Sample H2 contained only poorly-crystallised iron hydroxides; in sample HC located between HC3 and HC4, however, clay particles and pyrite crystals were observed (Figure 4). As it is not common to observe floating pyrite particles, the first analysis of sample HC was repeated (existing sample was filtered using a 45μ filter and re-analysed) four weeks after the first analysis. The results shown in Figure 4 confirmed the findings of the first analysis.

Framboids (spherical structures of crystals) of pyrite were found in both suspended matter and bottom sediments. In both these materials, the size varied between 5 and $20\mu\text{m}$; micro-framboids were also found and are generally $< 1\mu\text{m}$. There are several indications that pyrite was present in the creek water: 1) the physical appearance of the framboid, 2) the stoichiometry (gained by EDS microanalysis showing ~ 45% Fe and 55% S) was that of pyrite, and 3) pyrite was positively identified in the bottom sediments by XRD (1-2.6%).

The SEM analysis of pyrite found in suspended particulate matter shows two distinctive morphologies: firstly, loosely packed framboids that have an organic infilling or matrix between the individual spheres (Figure 4a); this structure allows physical disintegration of the framboid (e.g. Skei, 1988), and secondly, spherical clusters of well-formed microcrystals (Figure 4b and 4c).

In bottom sediments, closely packed spherical clusters of rounded microcrystals were absent. Only loosely packed framboids (Figures 5, 6 and 7) and single euhedral crystals of pyrite were found (Figure 8). The octahedral form of pyrite is usually scarce in recent sediments and is indicative of slow crystal growth. The formation of framboids, in contrast, is comparatively more rapid and it takes place under conditions of lower pH and higher Eh, and when supersaturated pyrite is able to nucleate rapidly onto suitable surfaces (Butler and Rickard, 2000).

The close spatial association of pyrite framboids and euhedra observed in bottom sediments in this study and elsewhere (e.g. Sawlowicz, 2000) may be due to their genetic relationship; it is possible there has been recrystallisation from framboidal to single grain pyrite (e.g. Love and Amstutz, 1966). Therefore, the presence of euhedral pyrite in bottom sediments of Halls Creek may be indicative of geochemical stability and a minimum degree of disturbance, which has enabled the slow crystal development of framboids to the euhedral form of pyrite.

In summary, the form and degree of packing of pyrite crystals is as follows: a) loosely packed framboids, mostly 5-20 μm , were found in bottom sediments and suspended matter, b) closely packed framboids were only found in suspended matter, and c) the rare euhedral form was only found in bottom sediments. The euhedral pyrite found in bottom sediments suggests that the formation and recrystallisation of pyrite is an ongoing process in the estuarine sediments.

As the oxygen concentration of the lower estuary water was high and well above 50 $\mu\text{mol/L}$ (e.g. Middelburg et al., 1988), the pyrite framboids could not have formed in the water column and are most likely eroded and mobilised from bottom or bank sediments. The presence of pyrite framboids in the suspended sediment suggests that estuarine water is unable to rapidly oxidise this mineral. This is most likely because silica and clay-rich gels (Fig 6a and 7, respectively) coat most of the suspended framboids, apparently delaying their oxidation (e.g. Middelburg et al., 1988) as well as enabling them to float.

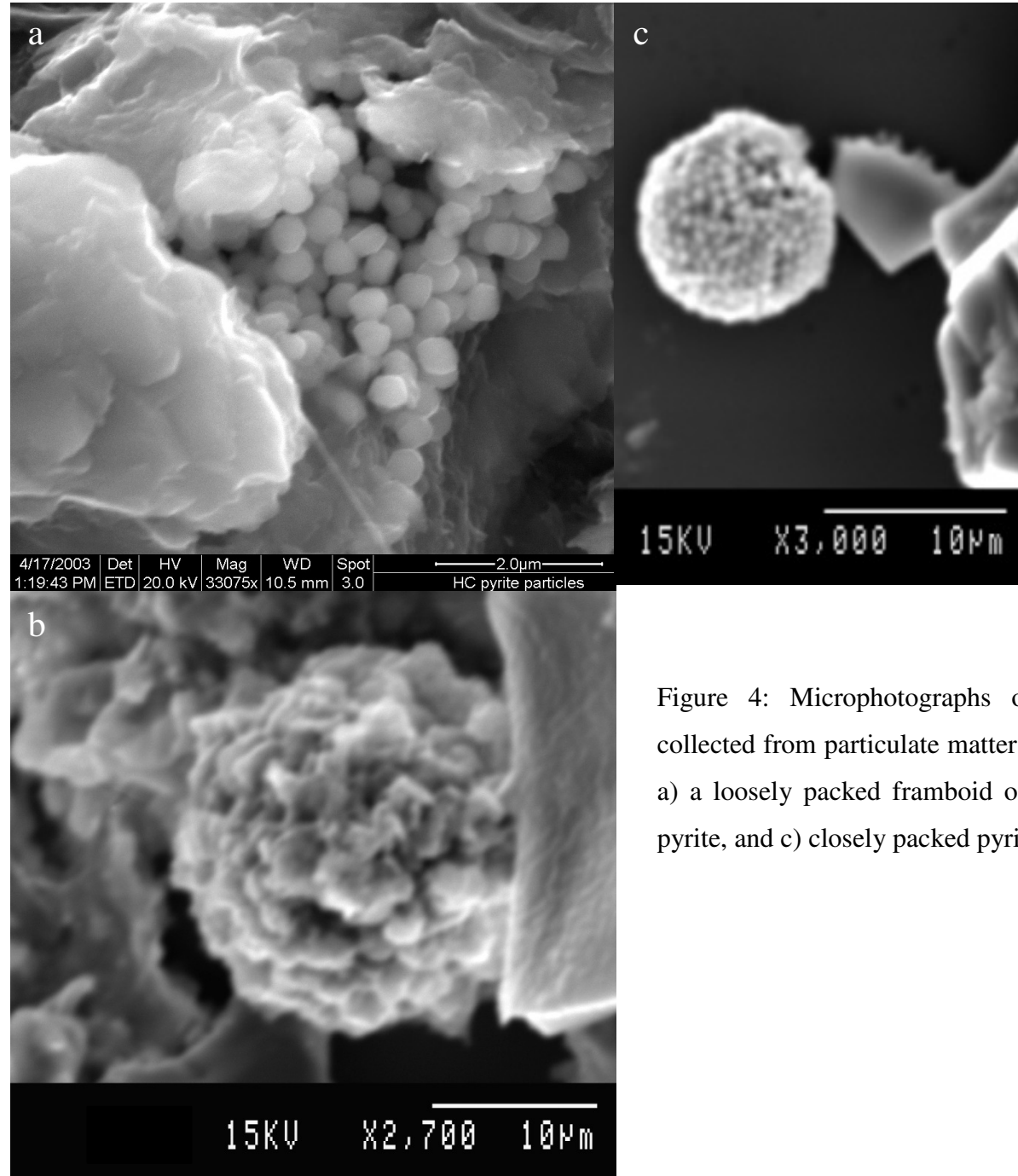


Figure 4: Microphotographs of framboidal pyrite crystals collected from particulate matter in the lower estuary (site HC): a) a loosely packed framboid of pyrite, b) poorly crystallised pyrite, and c) closely packed pyrite framboid.

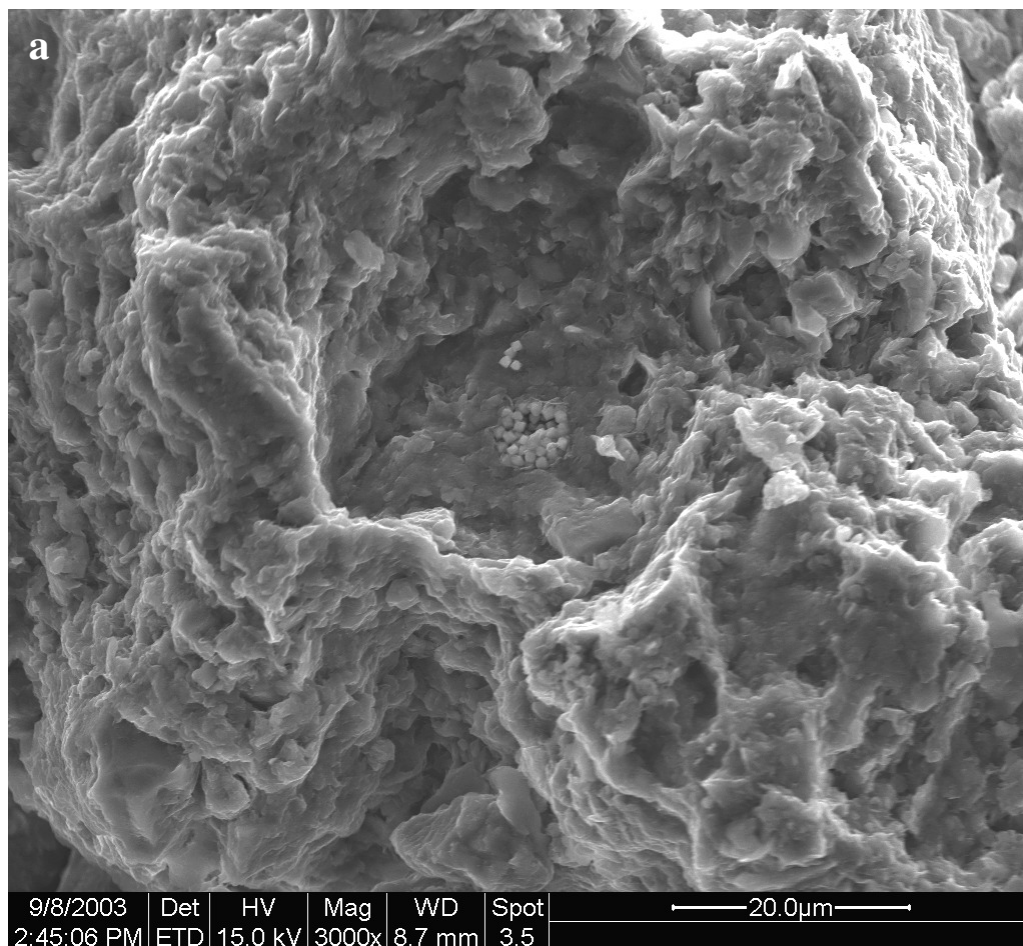
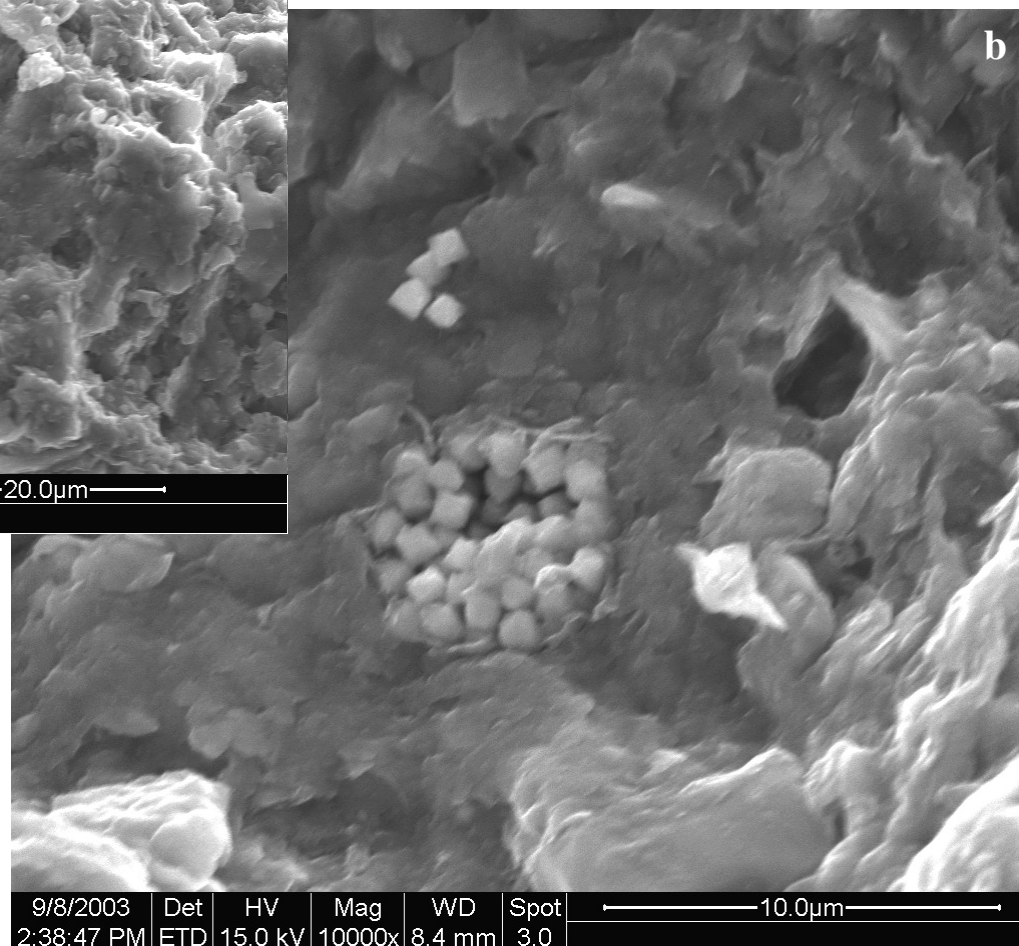


Figure 5: Bottom sediments at site HC3. The loose packing of the framboids suggests the presence of an organic infilling or matrix between the individual spheres (e.g. Skei, 1988).



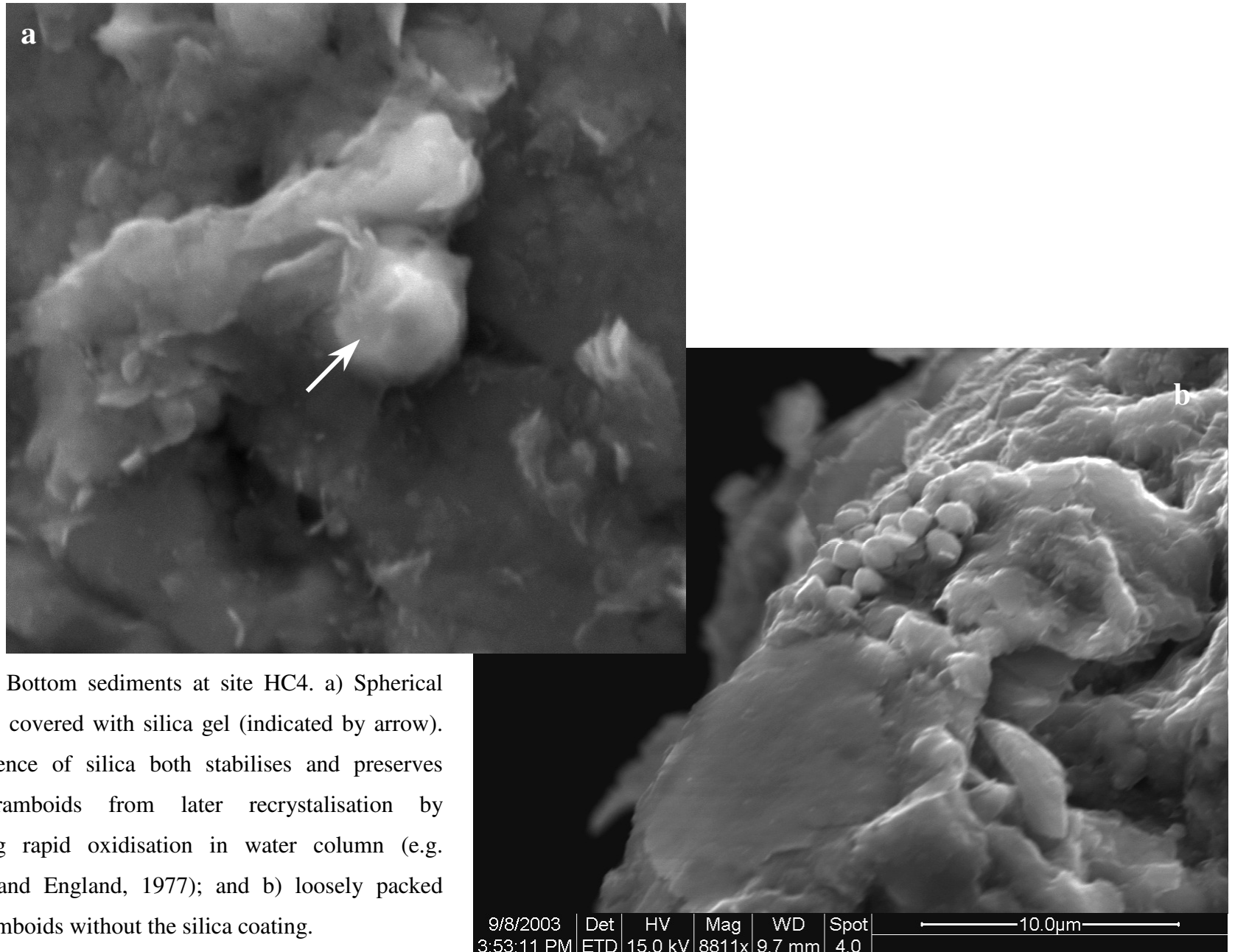


Figure 6: Bottom sediments at site HC4. a) Spherical framboids covered with silica gel (indicated by arrow). The presence of silica both stabilises and preserves pyrite framboids from later recrystallisation by preventing rapid oxidation in water column (e.g. Ostwald and England, 1977); and b) loosely packed micro-framboids without the silica coating.

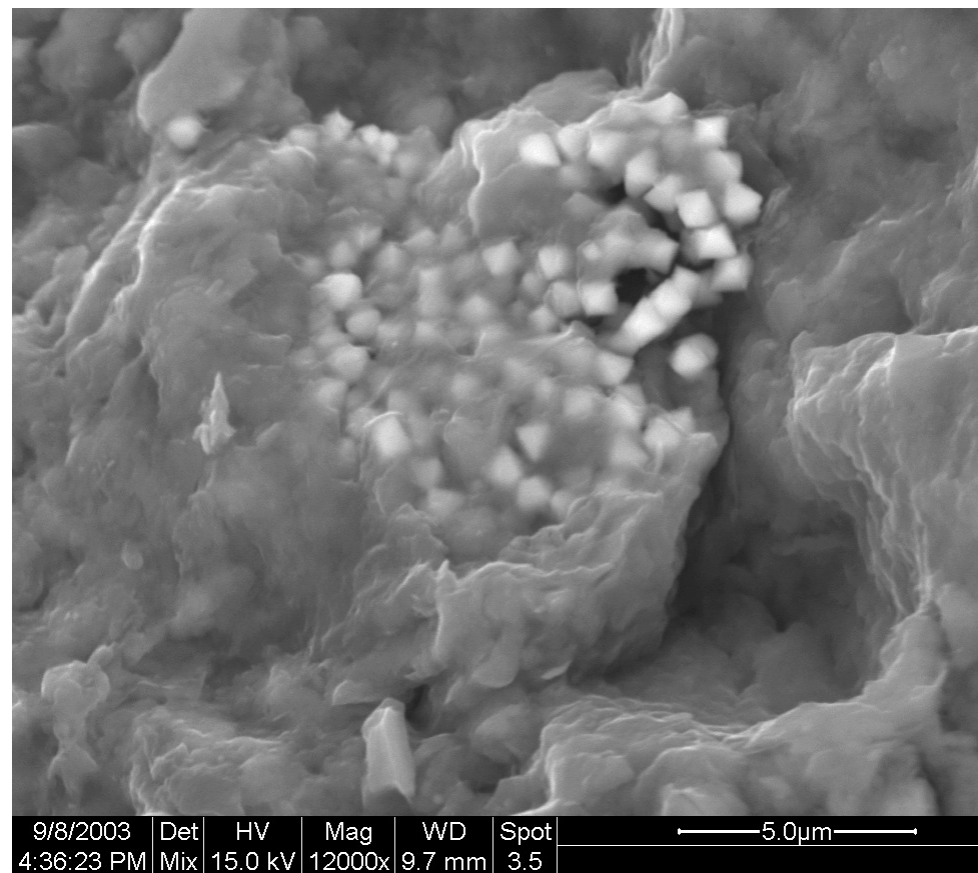


Figure 7: Micro-framboids, <1mm at site HC4, covered by a clayey gel (smectite stoichiometry was identified by EDS)

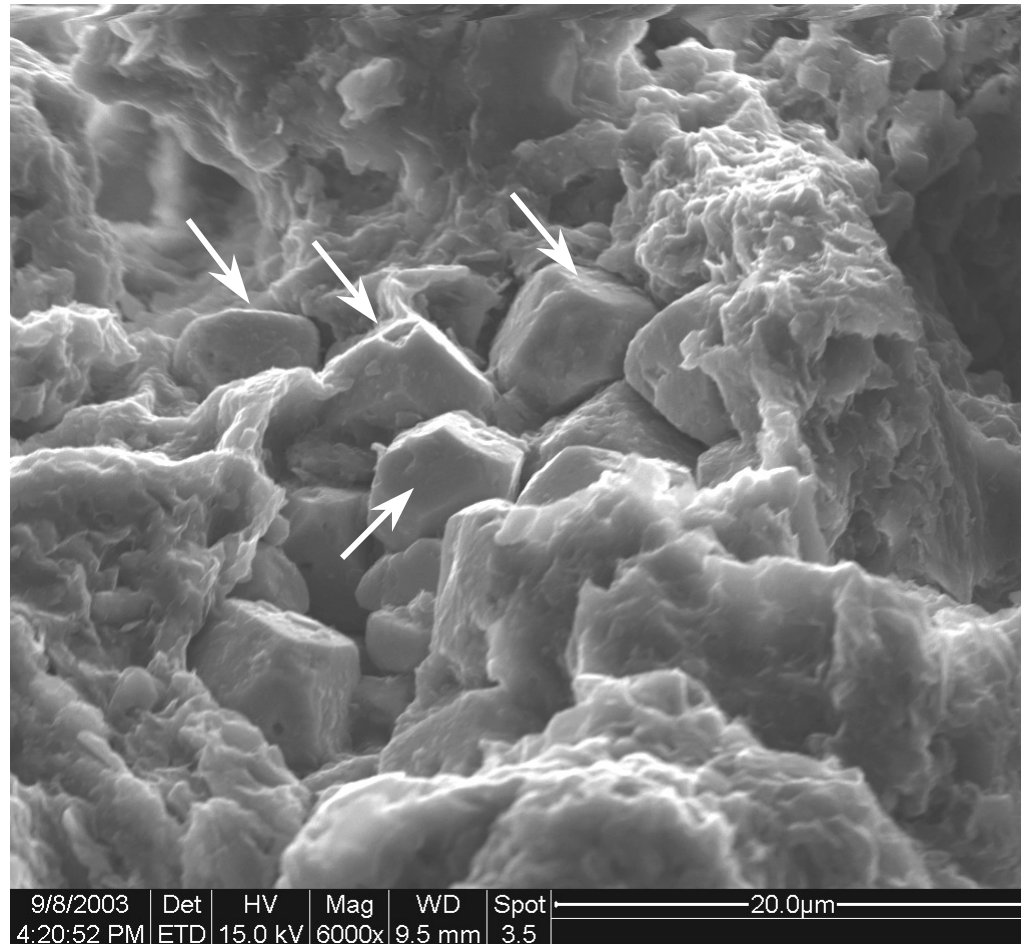


Figure 8: Arrowheads point to well-developed euhedral pyrite formed in bottom sediments in the lower estuary (HC4). Close spatial association of pyrite framboids and euhedra is common in natural settings and suggests a genetic relationship (Sawlowicz, 2000). The formation of euhedra is indicative of slow crystallisation.

4. Conclusions

The analysis of waters and bottom sediments from the Halls Creek catchment allows the following conclusions to be drawn:

1. While both evaporation and weathering were found to be major processes that control the major element geochemistry of water samples, the contribution of atmospheric precipitation is zero in all water samples.
2. Conductivity ranges widely from very fresh to saline, while pH has a relatively narrow range between slightly acid to slightly alkaline. Manganese and Al occur in very low concentration in water while the concentration of iron is high, with a maximum concentration of 15.7 mg/L.
3. The main primary minerals found in stream and estuarine bottom sediments are quartz and feldspars. The most abundant clay mineral present is kaolinite (up to 53%), followed by illite-smectite mixed layer and illite. Pyrite and hematite are also present in the bottom sediments. Iron released from adjacent areas during weathering precipitates as hematite in the fresher water section of Halls Creek. In contrast, in the estuarine reaches, anaerobic degradation of organic matter in bottom sediments results in the reduction of hematite; the resulting Fe^{2+} , in combination with sulfate from seawater and high loadings of organic matter, appears to be producing conditions favourable for the formation of pyrite in the estuarine substrate.
4. Pyrite was identified as part of a floating film of suspended sediment in the estuary. These sediments could have originated from erosion of streambed or bank, especially during rain events, which are known to increase the turbidity of the creeks in the region. The high oxygen content of the water confirmed that the pyrite framboids had not formed in the water column. Although framboidal morphology was dominant at all the sites, perfectly spherical closely packed framboids were only observed in the samples of suspended sediment. The rare octahedral form was present in bottom sediments, which indicates the slow *in situ* crystallisation of the pyrite and a minimum degree of disturbance of the substrate.

Acknowledgements The authors would like to thank Lensworth Group Ltd for financial support of the research. We thank Faculty of Science staff for assistance: Dr Thor Bostrom and Loc Duong (scanning electron microscopy), Wathsala Kumar (chemical analyses) and Tony Raftery (XRD analyses). Authors also thank Hayden McDonald from Mipela for the GIS database, and Tim Ezzy and Rob King for assisting with fieldwork. We gratefully acknowledge the anonymous reviewer of the manuscript for his valuable comments and suggestions.

References:

- Ahern KS, Udy J, O'Neil JM, Pointon S, Moody P, Albert S. Assessing the contribution of runoff and groundwater nutrients to toxic cyanobacteria blooms in southeast Queensland estuaries: a bioassay technique. In: River Symposium 2003, Urban Rivers, Balancing the Expectations, Brisbane, 2-5 September 2003, pp 10.
- Aston SR. Estuarine chemistry. In chemical oceanography (Riley JP, Chester R. eds.), New York, Academic Press 1978, pp. 361-440.
- Bache BW. Aluminium mobilisation in soils and waters. Jour of Geol Soc 1986, 143: 699-706.
- Berner RA. Sedimentary pyrite formation: An update. Geochim Cosmochim Acta 1984, 48: 605-615.
- Berner EK, Berner RA. Global Environment: water, air and geochemical cycles. New Jersey, Prentice Hall 1996, pp 376.
- Boyle EA, Edmond JM, Sholkovitz ER. The mechanism of iron removal in estuaries. Geochim Cosmochim Acta 1977, 41: 1313-1324.
- Burton JD. River borne materials and the continent-ocean interface. In physical and chemical weathering in geochemical cycles (Lerman A, Meybeck M. eds.) Dordrecht: The Netherlands, Kluwer 1988, pp 299-321.
- Butler IB, Rickard D. Framboidal pyrite formation via the oxidation of iron (II) monosulfide by hydrogen sulfide. Geochim Cosmochim Acta 2000, 64(15): 2665-2672.
- Canfield DE. Reactive iron in marine sediments. Geochim et Cosmochim Acta 1989, 53: 619-632.

- Canfield DE. Factors influencing organic carbon preservation in marine sediments. *Chem Geol* 1994, 114: 315-329.
- Canfield DE, Jorgensen BB, Fossing H, Glud R, Gundersen J, Ramsing NB, Thamdrup B, Hansen W, Nielsen LP, Hall POJ. Pathways of organic carbon oxidation in 3 continental margin sediments. *Mar Geol* 1993a, 113: 27-40.
- Canfield DE, Thamdrup B, Hansen W. The anaerobic degradation of organic matter in Danish coastal sediments – iron, manganese and sulfate reduction. *Geochim Cosmochim Acta* 1993b, 57: 3867-3883.
- Crerar DA, Means JL, Yuretic RF, Borcsik MP, Amster JL, Hastings DW, Knox GW, Lyon KE, Quiett RF. Hydrogeochemistry of the New Jersey coastal plain, transport and deposition of iron, aluminum, dissolved organic matter, and selected trace elements in stream, ground and estuary water. *Chem Geol* 1981, 33: 23-44.
- Croot PL, Hunter KA. Labile forms of iron in coastal seawater: Otago Harbour, New Zealand *Mar. Freshwater Res* 2000, 51: 193-203.
- Dennison WC, Albal EG. Moreton Bay study: a scientific basis of the healthy waterway campaign. Brisbane, southeast Queensland Regional Water Quality Management Strategy 1999, pp 245.
- Dent, D. and Pons, L. A world prospective on acid sulfate soils. *GEDMAB* 1995, 67: 263-176.
- Edmunds WM, Smedley PL. Groundwater geochemistry and health: an overview. In environmental geochemistry and health (Appleton JD, Fuge R, McCall GJH, eds.) *Geol Soc* 1996, 113: 91-105.
- Ezzy TR and Cox ME. Implications of land-use changes on groundwater within shallow coastal plain aquifers, Bells Creek catchment, southeast Queensland, Australia. In: Lopez-Geta JA and others (eds), *Coastal Aquifers Intrusion Technology: Mediterranean Countries: Contribution to our knowledge of the situation concerning marine water intrusion into Mediterranean coastal aquifers. Hidrogeologia Y Aguas Subterraneas N° 8*. Instituto Geologico Y Minero de Espana, 11-14 March 2003, Alicante, Spain, pp. 439-444.
- Faure G. Principles and application of geochemistry. New Jersey, Prentice Hall 1998 pp 600.

- Gibbs RJ. Mechanisms controlling world water chemistry. *SCI* 1970, 170: 1088-1090.
- Gorrell HA. Classification of formation waters based on sodium chloride content. *Amer Assoc Pet Geol Bull* 1953, 42(10): 2513.
- Greenberg AE, Clesceri LS, Easton AD, (eds.). Standard methods for the examination of water and wastewater, Washington D.C., American Public Health Association (APHA), American Water Works Association (AWWA), Water Pollution Control Federation (WPCF), 18th Edition 1992, pp 1-44.
- Jorgensen BB. The sulfur cycle of a coastal marine sediment (Limfjorden, Denmark). *Limnol and Oceanogr* 1977, 22: 814-832.
- Kuma K, Katsumoto A, Nishioka, J, Matsunaga K. Size-fractionated iron concentrations and Fe (III) hydroxide solubilities in various coastal waters. *Estuar, Coast Shelf Sci* 1998, 47: 275-283.
- Liaghati T, Preda M and Cox ME. Determination of Quaternary sediment sources using mineralogy and geochemistry in Bells Creek catchment, Pumicestone Passage, southeast Queensland. In Preiss VP (ed) *Proceedings of the International Conference on Geoscience: Expanding Horizons*, Adelaide 2002, Geological Society of Australia Incorporated, p 457.
- Liaghati T, Preda M, Cox ME. Heavy metal distribution and controlling factors within coastal plain sediments, Bells Creek catchment, southeast Queensland, Australia. *Environ Int* 2003, 29: 935-948.
- Liss PS. Conservative and non-conservative behaviour of dissolved constituents during estuarine mixing. In *estuarine chemistry* (Burton JD, Liss PS, eds). New York, Academic Press 1976: 93-130.
- Liu WX, Li XD, Shen ZG, Wang DC, Wai OWH, Li YS. Multivariate statistical study of heavy metal enrichment in sediments of the Pearl River Estuary. *Environ Pollut* 2003, 121: 377-388.
- Lord CJ, Church TM. The geochemistry of salt marshes: sedimentary ion diffusion, sulfate reduction and pyritisation. *Geochim Cosmochim Acta* 1983, 47: 1381-1391.
- Loring DH, Rantala RTT. Manual for geochemical analyses of marine sediments and suspended particulate matter. *Earth – Sci Rev* 1992, 32: 235-283.

- Love LG, Amstutz GC. Review of microscopic pyrite from the Devonian Chattanooga shale and Rammelsberg Banderz. *Fortschr Mineral* 1966, 43: 273-309.
- Martin JH, Fitzwater SE, Gorson RM. Iron deficiency limits phytoplankton growth in Antarctic waters. *Biogeochem Cycl* 1990, 4: 5-12.
- Martin JM, Windom HL. Present and future roles of ocean margins in regulating marine biogeochemical cycles of trace elements. In *ocean marginal processes in global change* (Montora RFC, Martin JM, Wollast R, eds) UK, Wiley 1991, pp. 45-68.
- Middelburg JJ, de Lange GJ, van der Sloot HA, van Emburg PR, Sophiah S. Particulate manganese and iron framboids in Kau Bay, Halmahedra (eastern Indonesia). *Mar Chem* 1988, 23: 353-364.
- Morel FMM, Hering JG. *Principles and applications of aquatic chemistry*. New York, Wiley-Interscience 1993, pp. 588.
- NSR Environmental Consultants. Caloundra Downs informal land use investigation: consolidated data report, main volume. Report prepared for Lensworth Group Limited 1999, Brisbane, Queensland.
- Ostwald J, England BM. Notes on framboidal pyrite from Allandale New South Wales, Australia. *Mineral Deposita* 1977, 12: 111-116.
- Pearl HW, Crocker KM, Prufert LE. Limitation of N₂ fixation and oxygenic photosynthesis in the nonheterocystous mat-forming cyanobacteria *Lyngbya*. *Appl Env Microbiol* 1987, 32: 525-536.
- Preda M, Cox ME. Sediment-water interaction, acidity and other water quality parameters in a subtropical setting, Pimpama River, southeast Queensland. *Environ Geol* 2000, 39 (3-4): 319-329.
- Preda M, Cox ME. Trace metal occurrence and distribution in sediments and mangroves, Pumicestone Region, southeast Queensland, Australia. *Environ Int* 2002, 28: 433-449.
- Rickard DT. Sedimentary iron sulfide formation. *Proceedings of the International Symposium on Acid Sulfate Soils*, 13-20 August 1972, Wageningen, The Netherlands 1973, Vol 1: 28-66.
- Rose AL, Waite TD. Kinetics of iron complexation by dissolved natural organic matter in coastal waters. *Mar Chem* 2003, in press.

- Sawlowicz Z. Framboids: from their origin to application. *Prace Mineral Pan* 2000, 88: 1-80.
- Skei JM. Formation of framboidal iron sulfide in the water of a permanently anoxic fjord-Framvaren, South Norway. *Mar Chem* 1988, 23: 345-352.
- Stumm W, Morgan JJ. *Aquatic chemistry: chemical equilibria and rates in natural waters*. 3rd Edition, New York, Wiley-Interscience 1996, pp. 1022.
- Swayze GA, Clark RN, Pearson RM, Livo KE. Mapping acid-generating minerals at the California Gulch superfund site in Leadville, Colorado using imaging spectroscopy. 6th Annual JPL Airborne Earth Science Workshop, March 4-8, 1996, Colorado, U.S. Geological Survey and U.S. Bureau of Reclamation.
- Wada H, Seisuwan B. The process of pyrite formation in mangrove soils. Selected papers of the Dakar Symposium on Acid Sulfate Soils, Dakar January 1986. International Institute for Land Reclamation and Improvement Publication 1988, pp. 44.
- Watkinson A. *Ecophysiology of the marine cyanobacterium, Lyngbya majuscula* (Honours thesis), Department of Botany, University of Queensland 2000.
- Wijsman JWM, Middelburg JJ, Heip CHR. Reactive iron in Black Sea sediments: implication for iron cycling. *Mar Geol* 2001, 172: 167-180.
- Zwolsman JJ, van Eck GTM, Burger G. Spatial and temporal distribution of trace metals in sediments from the Scheldt Estuary, South-west Netherlands. *Estuar Coast Shelf Sci* 1996, 43: 55-79.